ELSEVIER

Materials Science and Engineering A319–321 (2001) 63–73

MATERIALS SCIENCE & ENGINEERING A

www.elsevier.com/locate/msea

Orientation dependence of the cyclic deformation behavior and the role of grain boundaries in fatigue damage in copper crystals

Z.G. Wang *, Z.F. Zhang, X.W. Li, W.P. Jia, S.X. Li

State Key Laboratory for Fatigue and Fracture of Materials, Institute of Metal Research, The Chinese Academy of Sciences, 72 Wenhua Road, Shenyang 110015, People's Republic of China

Abstract

In this overview paper, the features and the occurrence of a plateau on the cyclic stress–strain curve in copper single crystals as well as the associated microstructural characteristics are summarized. Unified and comprehensive diagrams are provided. Grain boundaries (GBs) play an important role in fatigue cracking even at intermediate and low-strain amplitudes. However, the associated mechanisms still remain unclear. In the present studies, copper bicrystals, columnar crystals and tricrystals with different orientations were examined. By using the electron channeling contrast (ECC) technique in scanning electron microscopy (SEM), the interaction of persistent slip bands (PSBs) with GBs was clearly revealed. A modified intergranular fatigue cracking mechanism was suggested. The present investigations also disclosed the significant role of the grain boundary triple lines and triple junctions (TJs) in fatigue damage.

Keywords: Cyclic deformation; Cyclic stress–strain curve; Grain boundary; Persistant slip bands

1. Introduction

When a well-annealed Cu crystal suitably oriented for single slip is subjected to cyclic deformation between constant plastic strain amplitude limits γ_{pl} at room temperature in air, it will harden under the action of cyclic straining. The peak stress increases rapidly at first and then more slowly, approaching a value, the saturation stress τ_s. A plot of saturation stress τ_s versus the plastic strain amplitude γ_{pl} generates the 'cyclic stress–strain (CSS) curve'. Mughrabi [1] performed constant plastic strain amplitude tests on single-slip oriented Cu single crystals over a wide range of strain amplitudes and obtained a well-documented CSS curve which clearly demonstrated three regions marked by A, B and C. At region A ($\gamma_{pl} < 6 \times 10^{-5}$), work hardening occurs during cyclic loading and the microstructure is characterized by veins. Region A is followed by a strain-independent region B known as the 'plateau' where the dislocation configuration can be described as 'two-phase' structures: ladders and veins. This plateau region extends over two decades of plastic strain amplitude ($6 \times 10^{-5} < \gamma_{pl} < 7.5 \times 10^{-3}$). A further increase in plastic strain amplitude ($\gamma_{pl} > 7.5 \times 10^{-3}$) results in a continuous increase in the saturation stress named region C where cell or labyrinth structures associated with multiple slip may develop.

Similar to the stress–strain curve in monotonic loading, the CSS curve in cyclic loading is a basic property, which reflects numerous insight into a material's fatigue behavior. In particularly, the plateau region B is characterized by the formation of PSBs which frequently act as preferential sites for fatigue crack nucleation. Therefore, many researchers attempted to examine the crystallographic orientation dependence of the CSS curve of Cu. Cheng and Laird [2] measured the cyclic saturation stresses of Cu crystals with a very wide variety of orientations inside the stereographic triangle, including some near to its boundaries. All the crystals saturated remarkably near 29 MPa. Cheng and Laird, therefore, concluded that the cyclic saturation stress is independent of orientation. Later, some investigators carried out cyclic deformation tests by using double- or multiple-slip-oriented Cu single crystals where two or more slip systems are simultaneously excited [3–5]. However, no clear orientation dependence of CSS curves and the associated microstructures were reported by these inves-

* Corresponding author. Tel.: +86-24-23843531.
E-mail address: zhgwang@imr.ac.cn (Z.G. Wang).

0921-5093/01/$ - see front matter
PII: S0921-5093(01)01055-3

tigators because of limited and difficult experiments. Since then, research on this important topic has waned.

Most engineering materials are in polycrystalline forms. Compared with single crystals, our knowledge about the cyclic deformation mechanisms in Cu polycrystals is obviously much less. As for polycrystalline materials, there are at least three distinct important features that bring about their deformation behavior in a manner very different from single crystals oriented for single slip (1) many grains in a polycrystal will be in all kinds of double- or multiple-slip orientations; (2) grain boundaries with different orientations and structures will act as obstacle against slip deformation and act as fatigue crack nucleation sites and, furthermore; (3) due

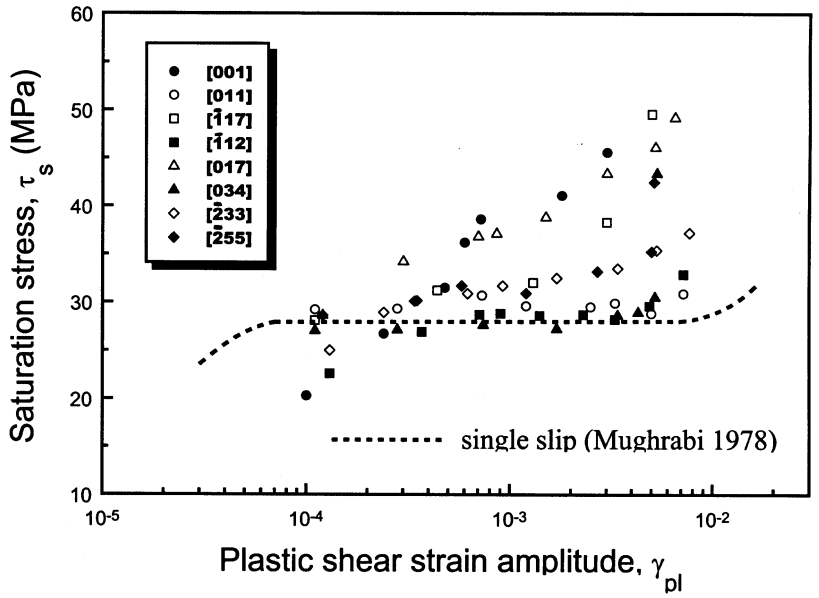

Fig. 1. Cyclic stress–strain curves of double- and multiple-slip-oriented Cu single crystals. The dashed line represents the result of single-slip-oriented crystals.

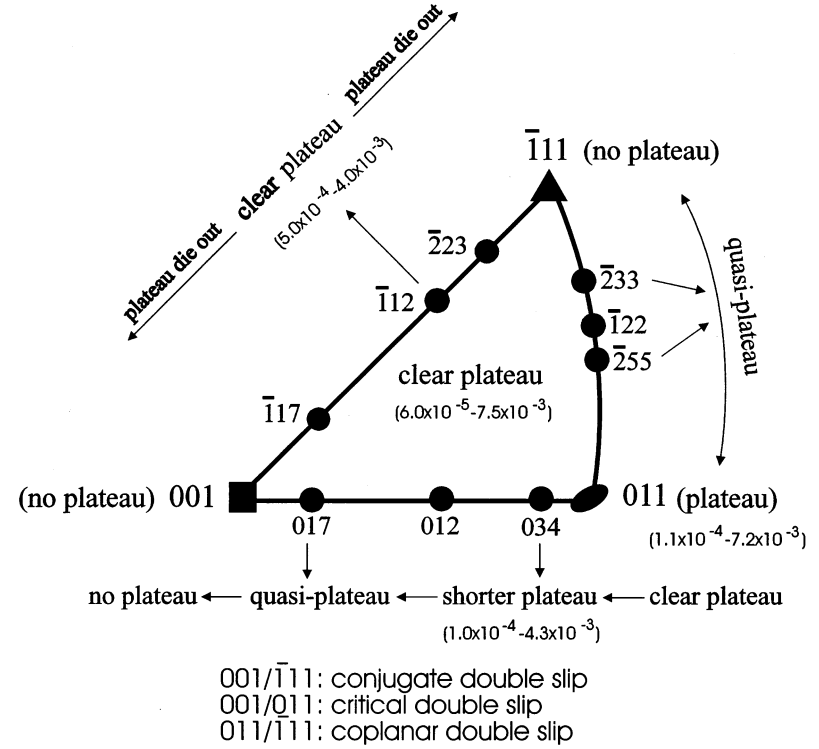

Fig. 2. Variation of the crystal CSS curves with its location in the standard stereographic triangle.

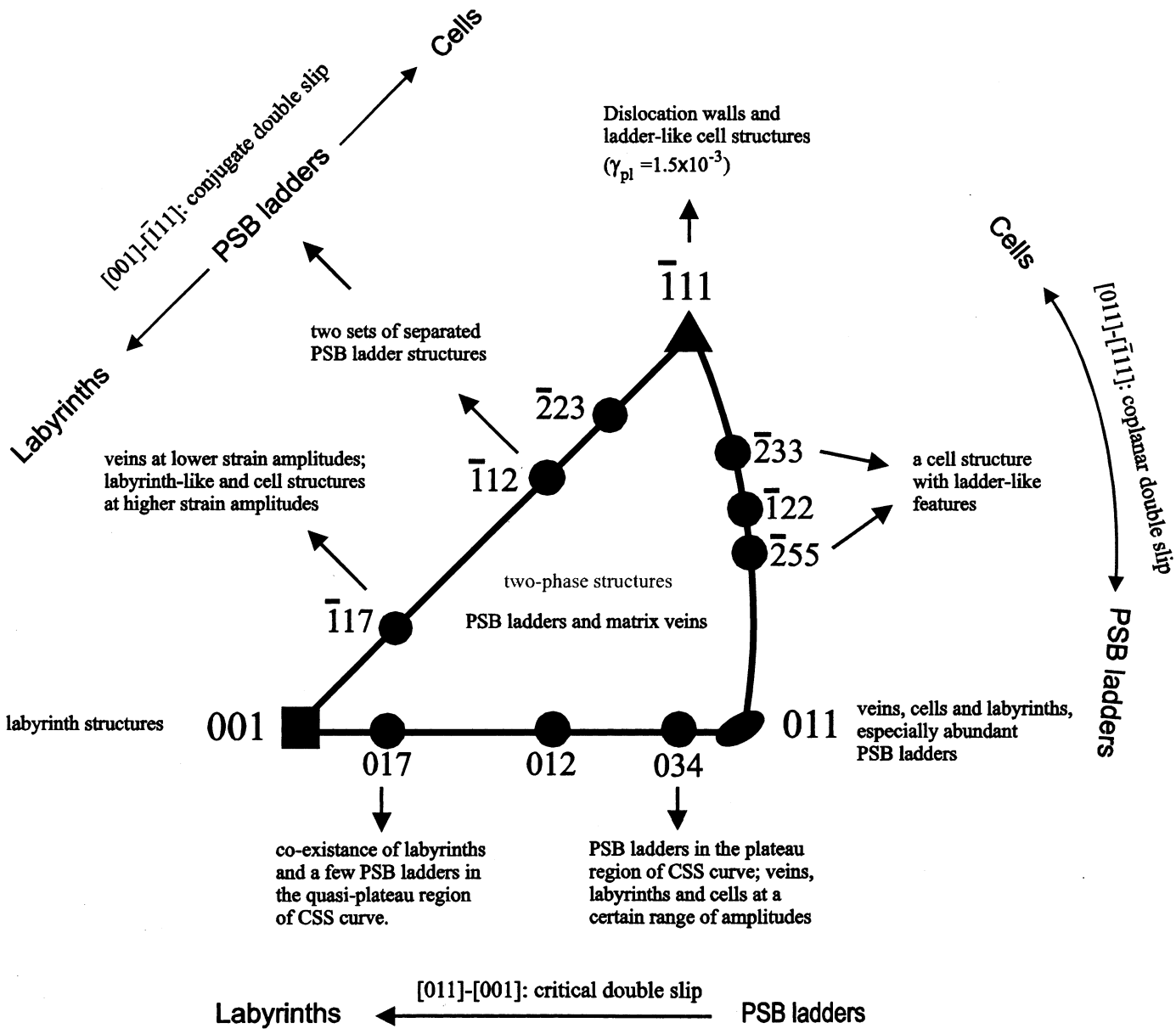

Fig. 3. Dependence of dislocation structures induced by cyclic deformation on the location of the examined crystals in the standard stereographic triangle.

to elastic as well as plastic deformation incompatibility between adjacent grains, it seems that all the grains in a polycrystalline sample are always subjected to an actual multiaxial loading conditions. Apparently, the connection between the cyclic response of mono- and polycrystalline material might not be as simple as previously suggested [6]. Recently, Laird pointed out [7] that a good model to extrapolate the cyclic behavior of polycrystals from that of a single crystal seems to be still out of reach.

In the present work, the cyclic deformation behavior of Cu single crystals oriented for double or multiple slip, bicrystals and tricrystals with different orientations were studied systematically.

2. Orientation dependence of CSS curves and the associated dislocation structures

Copper single crystal bars or plates were grown from OFHC Cu of 99.999% purity by the Czochralski or Bridgman method. A group of fatigue specimens oriented typically as [1̄ 1 7], [1̄ 1 2] and [2̄ 2 3] for conjugate double slip, [0 1 7] and [0 3 4] for critical double slip, [2̄ 5 5] and [2̄ 3 3] for coplanar double slip as well as [0 0 1], [0 1 1] and [1̄ 1 1] for multiple slip were carefully spark machined from the as-grown single crystal ingots. Three single-slip-oriented crystals [1̄ 3 5], [1̄ 2 5] and [4̄ 18 41] were also selected for comparison. Push–pull fatigue tests under plastic strain control were performed

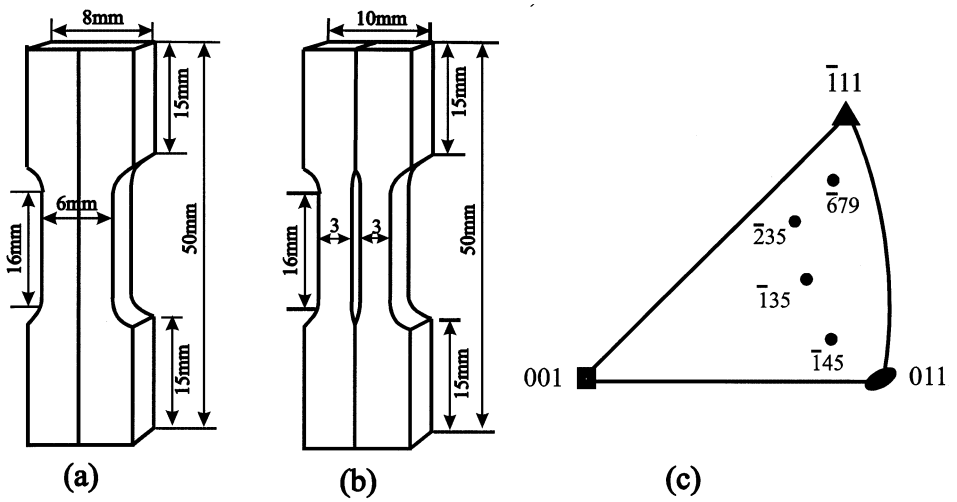

Fig. 4. Geometry of fatigue specimens of Cu bicrystal with GB parallel to loading axis. (a) RB type; (b) CB type; (c) orientations of component crystals.

at room temperature in air using servo-hydraulic machines. The CSS curves of double- and multiple-slip-oriented crystals are shown in Fig. 1. It can be seen that the orientation of the specimen not only affects the level of cyclic saturation stress, but also the shape of the CSS curve, especially its plateau region. According to the crystallographic orientation, the observed CSS curve can be roughly divided into three groups; (1) like that of single-slip-oriented crystals, the CSS curve shows a clear plateau, such as crystals [0 1 1], [0 3 4] and [$\bar{1}$ 1 2]; (2) there is no clear plateau on the CSS curve, but a quasi-plateau may exist within a certain range of strain amplitude, such as crystals [$\bar{2}$ 3 3] and [$\bar{2}$ 5 5], and (3) the saturation stress τ_s increases monotonously with increasing the strain amplitude. There is no plateau in the CSS curve, such as crystals [0 0 1], [$\bar{1}$ 1 7] and [0 1 7].

Based on our own experimental results and some available in literature, the effect of crystallographic orientation on the characteristics of CSS curves can be summarized in Fig. 2. The main points are; (1) for most orientations within the standard triangle, the shape of the CSS curve appears to be quite constant with a clear plateau regime over a wide strain range; (2) the CSS curve of [0 0 1], [$\bar{1}$ 1 1] crystals shows no plateau, but a clear plateau exists for [0 1 1] crystals; (3) [$\bar{1}$ 1 2] orientation which shows a clear plateau separates the 0 0 1/$\bar{1}$ 1 1 boundary into two parts. When the orientation of the specimen varies from [$\bar{1}$ 1 2] either towards [$\bar{1}$ 1 1] or [0 0 1], the plateau regime becomes shorter and finally disappears; (4) on the 0 1 1/0 0 1 boundary, when the orientation varies from [0 1 1] to [0 0 1], the shape of the CSS curve changes correspondingly, from one with a longer and clear plateau to one without any plateau, and with a shorter or quasi-plateau in between; (5) on the 0 1 1/$\bar{1}$ 1 1 boundary, the transition from a clear plateau for [0 1 1] crystals to no plateau for [$\bar{1}$ 1 1]

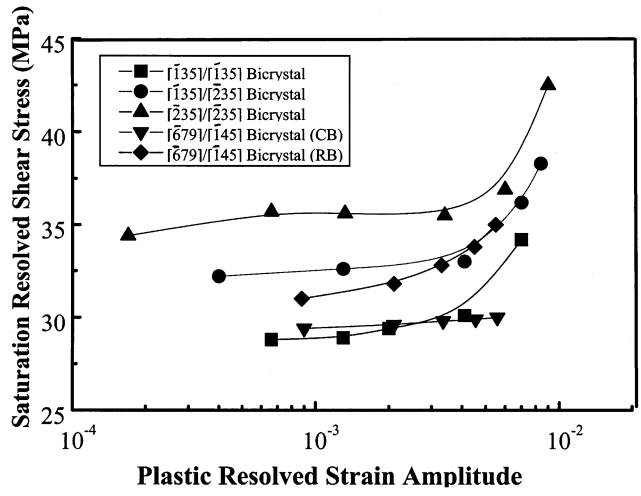

Fig. 5. CSS curves of RB type bicrystals [$\bar{1}$ 3 5]/[$\bar{1}$ 3 5], [$\bar{1}$ 3 5]/[$\bar{2}$ 3 5] and [$\bar{6}$ 7 9]/[$\bar{1}$ 4 5] and CB type bicrystal [$\bar{6}$ 7 9]/[$\bar{1}$ 4 5].

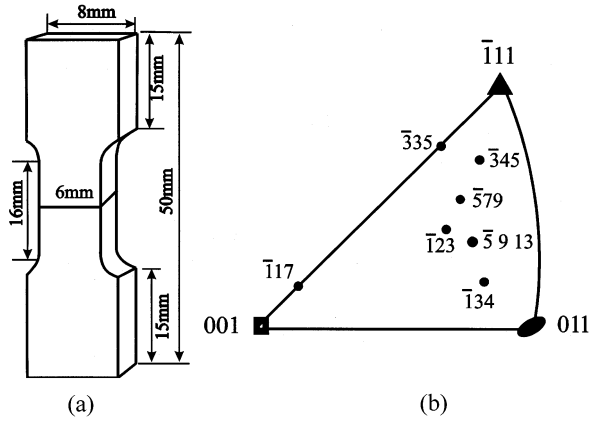

Fig. 6. Fatigue of Cu bicrystals with perpendicular GBs. (a) Geometry of fatigue specimens; (b) Orientations of component crystals.

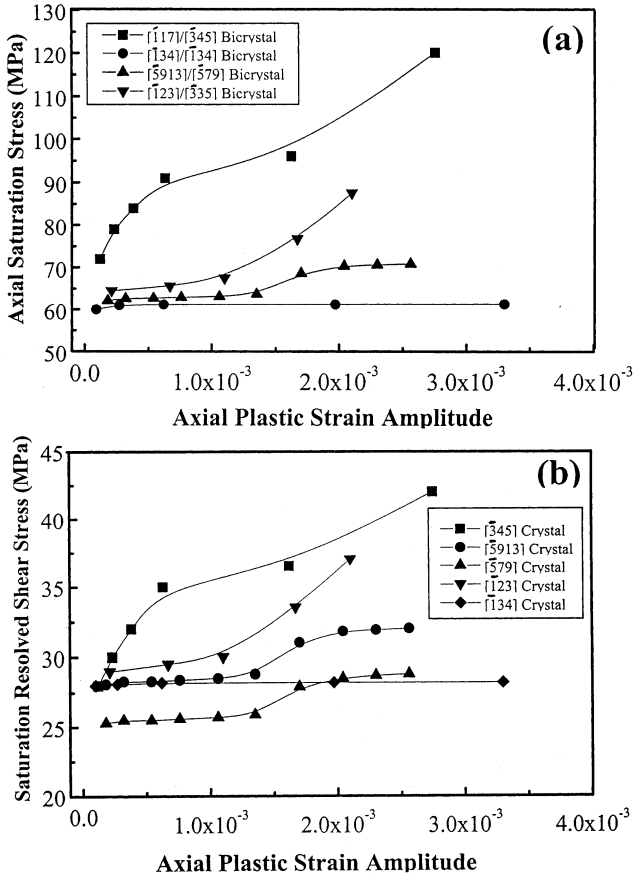

Fig. 7. The effect of component crystal orientation. (a) CSS curves of four bicrystals indicating the influence of component crystal orientations. (b) The relationship of resolved shear stress on primary slip plane with the axial strain amplitude.

crystals is characterized by a quasi-plateau for [$\bar{2}$ 5 5] and [$\bar{2}$ 3 3] crystals in between.

The dependence of CSS curves on the crystallographic orientation can well be rationalized in terms of the dislocation structures induced by dislocation reactions through single, double and multiple slip. Fig. 3 schematically summarizes the cyclic deformation induced dislocation configurations in crystals located in the different areas of the standard stereographic triangle. It can be easily seen that there exists a reasonable consistency between Fig. 2 and Fig. 3.

3. Roles of grain boundaries (GBs) in fatigue damage

The fatigue damage in polycrystalline materials is affected by many factors, such as grain size, grain boundary structures, misorientation between grains, strain amplitude, texture and so on. Grain boundaries are supposed to be one of the most important factors leading to fatigue damage. Bicrystals consisting of well-designed component grains can be regarded as good model materials for studying fatigue damage of polycrystalline materials. In the present work, the fatigue damage of Cu bicrystals with GB either parallel or perpendicular to the stress axis, or inclined relative to the loading axis was investigated.

3.1. Cyclic stress–strain response of bicrystals with parallel GB

Fig. 4(a) shows the geometry of fatigue specimens of Cu bicrystals with GB parallel to the loading axis. They are referred to as RB type bicrystals [$\bar{1}$ 3 5]/[$\bar{1}$ 3 5], [$\bar{1}$ 3 5]/[$\bar{2}$ 3 5], [$\bar{2}$ 3 5]/[$\bar{2}$ 3 5] and [$\bar{6}$ 7 9]/[$\bar{1}$ 4 5]. Fig. 4b is the same bicrystal as RB type [$\bar{6}$ 7 9]/[$\bar{1}$ 4 5], but the grain boundary in the gauge length was scooped to avoid the GB effect and is referred to as CB type. The crystallographic orientations of all the component crystals in the bicrystals are shown in Fig. 4c, indicating they are all single-slip-oriented. The CSS curves of all the bicrystals are shown in Fig. 5. It can be seen that all bicrystals except RB [$\bar{6}$ 7 9]/[$\bar{1}$ 4 5] exhibited CSS curves with a plateau. But the plateau stresses are quite different, indicating the difference in GB strengthening. Since the orientation of [$\bar{2}$ 3 5] is close to double slip, it is believed that the activation of secondary slip owing to

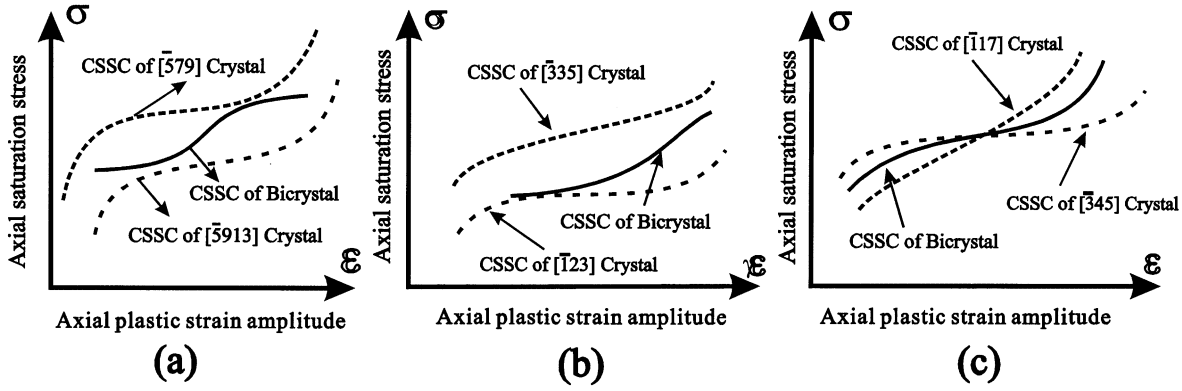

Fig. 8. Schematic illustrations of the combination of CSS curves of the two component crystals in bicrystals with perpendicular GBs. (a) [$\bar{5}$ 9 1 3]/[5 7 9]; (b) [$\bar{1}$ 2 3]/[$\bar{3}$ 3 5]; and (c) [$\bar{3}$ 4 5]/[$\bar{1}$ 1 7].

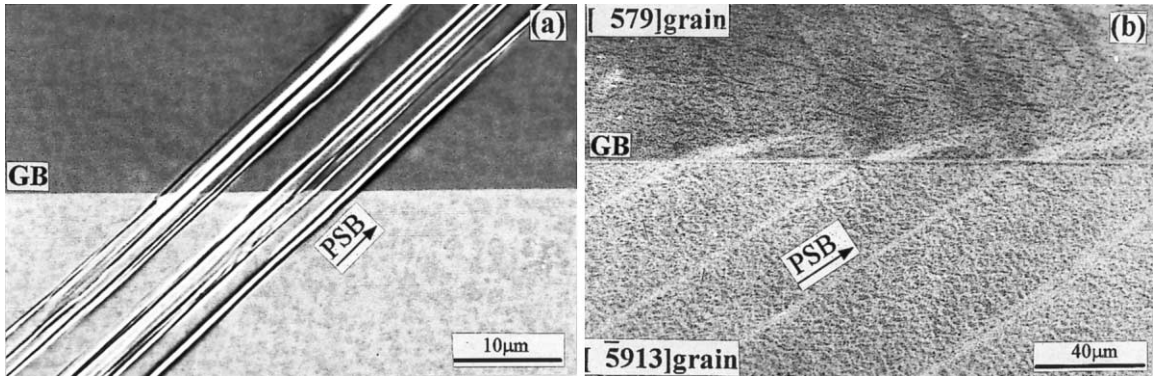

Fig. 9. Interactions of PSBs with low-angle GBs at $\gamma_{pl} = 6.4 \times 10^{-4}$ (a) and with large-angle GBs at $\gamma_{pl} = 7.6 \times 10^{-4}$ (b).

the constraint of the GB is responsible for the increase in the plateau stress of bicrystals [$\bar{1}$ 3 5]/[$\bar{2}$ 3 5] and [$\bar{2}$ 3 5]/[$\bar{2}$ 3 5]. The fact that the cyclic saturation stress of the RB type [$\bar{6}$ 7 9]/[$\bar{1}$ 4 5] is higher than that of CB type [$\bar{6}$ 7 9]/[$\bar{1}$ 4 5] is a clear indication of the GB affected zone on cyclic hardening.

Chuang and Margolin [8] roughly estimated the stress increment due to the GB affected zone for β-brass bicrystals under monotonic loading as

$$\sigma_T = \sigma_B + V_{GB}(\sigma_{GB} - \sigma_B) \quad (1)$$

where σ_T is the applied tensile stress, σ_B is the stress acting on the component crystal, V_{GB} is the volume fraction of GB affected zone, and σ_{GB} is the stress increment induced by GB affected zone. In the present case, taking CB type bicrystal [$\bar{6}$ 7 9]/[$\bar{1}$ 4 5] and RB type bicrystal [$\bar{6}$ 7 9]/[$\bar{1}$ 4 5] as example for comparison, we have

$$\sigma_{CB} = \sigma_{G1} V_{G1} + \sigma_{G2} V_{G2} \quad (2)$$

where σ_{CB} is the cyclic saturation stress of [$\bar{6}$ 7 9]/[$\bar{1}$ 4 5](CB), σ_{G1} and σ_{G2} are cyclic saturation stresses of component crystal G1 and G2, respectively. V_{G1} and V_{G2} are volume fractions of G1 and G2, respectively. Taking the effect of GB into account for [$\bar{6}$ 7 9]/[$\bar{1}$ 4 5] and using the similar form of Eq. (1), it is straightforward to obtain the following expression

$$\sigma_{RB} = \sigma_{CB} + V_{GB}(\sigma_{GB} - \sigma_{CB}) \quad (3)$$

The average saturation stress in the GB affected zone σ_{GB} is

$$\sigma_{GB} = \frac{\sigma_{RB} - \sigma_{CB}}{V_{GB}} + \sigma_{CB} \quad (4)$$

Since the applied stresses σ_{RB} and σ_{CB} are all known, if the volume fraction V_{GB} of GB affected zone is measured, σ_{GB} can be easily calculated. A good relationship between σ_{GB} and V_{GB} has been obtained experimentally.

3.2. Cyclic deformation of bicrystal with perpendicular GB

In polycrystalline materials, GB orientations with respect to the loading axis are randomly distributed. In order to further understand GB effect on fatigue damage in polycrystals, it is necessary to study bicrystals with GBs at different angles to the loading axis.

In polycrystals, GBs perpendicular to the loading axis often exist. However, perpendicular GBs have been seldom studied because of some difficult analysis in mechanics. When a bicrystal with a perpendicular GB is

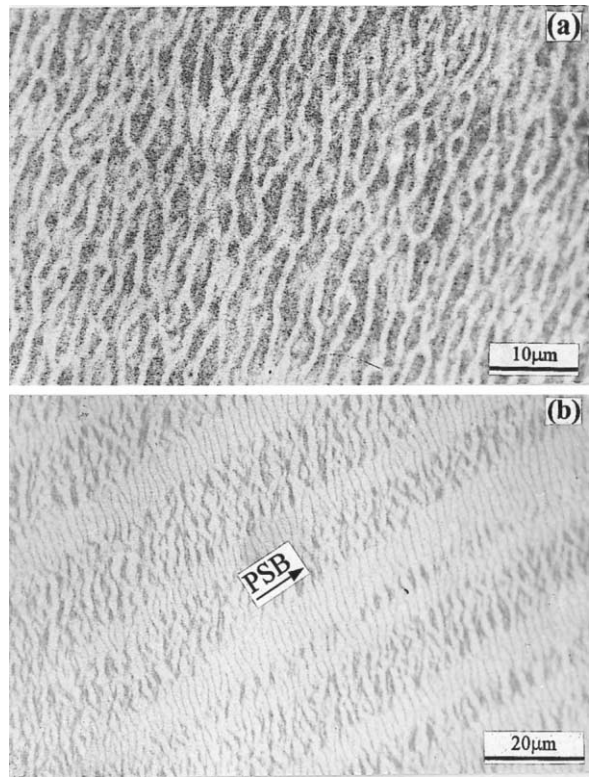

Fig. 10. Spatial distribution of dislocation configurations induced by cyclic deformation on a common primary slip plane of two grains. (a) Typical dislocation veins; (b) Beneath the vein structures are PSB ladders embedded in the veins.

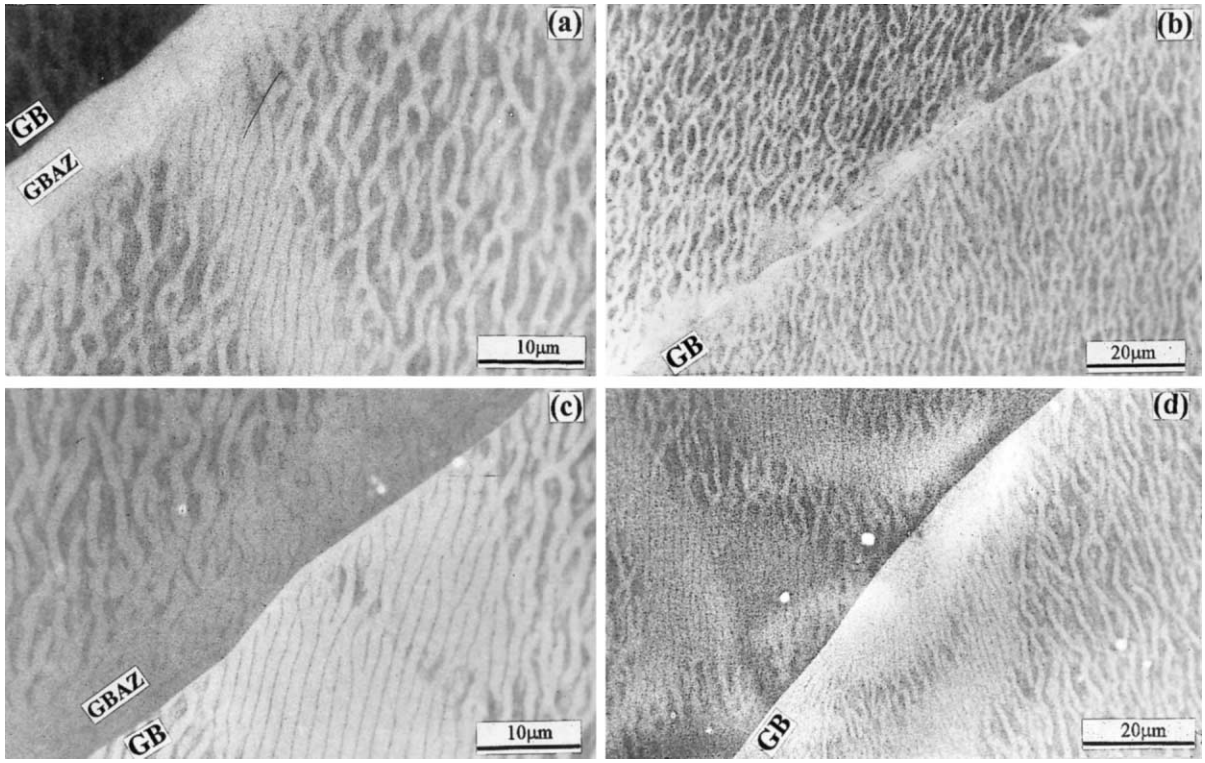

Fig. 11. Dislocation patterns near the GB on a common primary slip plane in a bicrystal. (a) The appearance of GBAZ away from the specimen center; (b) the disappearance of GBAZ at the center of the specimen; (c), (d) interaction of PSB walls with the GB.

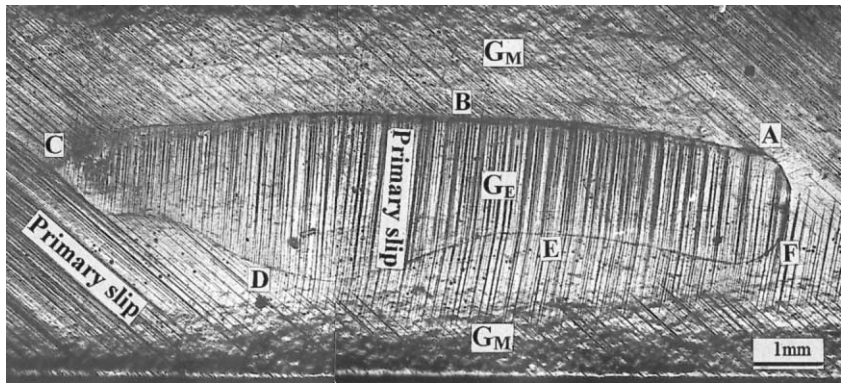

Fig. 12. Optical micrograph, indicating the surface slip morphology of a Cu crystal G_M with an embedded small grain G_E after fatigue loading.

loaded, the strain distribution among the consisting components strongly depends on the Schmid factor of the component crystals. The two components in the bicrystal may carry quite different strain during cyclic loading. This fact makes the problem more difficult to be analyzed. Peralta and Laird [9,10] studied the cyclic deformation of Cu bicrystals [0 0 1]/[$\bar{1}$ 4 9] with perpendicular GBs. They found that the softer component crystal [$\bar{1}$ 4 9] in bicrystal [0 0 1]/[$\bar{1}$ 4 9] carried about 80% of the total applied strain amplitude. This means that the orientation difference of the components may play more important role than GB itself. In the present work, four types of bicrystals with perpendicular GBs [$\bar{3}$ 4 5]/[$\bar{1}$ 1 7], [$\bar{1}$ 3 4]/[$\bar{1}$ 3 4], [$\bar{5}$ 9 1 3]/[$\bar{5}$ 7 9] and [$\bar{1}$ 2 3]/[$\bar{3}$ 3 5] were produced for study. In Fig. 6a and b are shown the geometry of fatigue specimens and the orientation of component crystals. Fig. 7a shows the CSS curves of four bicrystals demonstrating the strong influence of component crystal orientations. Bicrystal [$\bar{1}$ 3 4]/[$\bar{1}$ 3 4] has the lowest saturation stresses and showed a clear plateau in its CSS curve. As compared with [$\bar{1}$ 3 4]/[$\bar{1}$ 3 4], bicrystal [$\bar{5}$ 9 1 3]/[$\bar{5}$ 7 9] exhibited higher saturation stresses and two plateau regions in the CSS curves. As for bicrystal [$\bar{1}$ 2 3]/[$\bar{3}$ 3 5], the saturation stresses became higher than that of [$\bar{5}$ 9 1 3]/[$\bar{5}$ 7 9] and there was only a short plateau in the CSS curve. Bicrystal [$\bar{3}$ 4 5]/[$\bar{1}$ 1 7] showed the highest cyclic saturation stresses among the four bicrystals and a

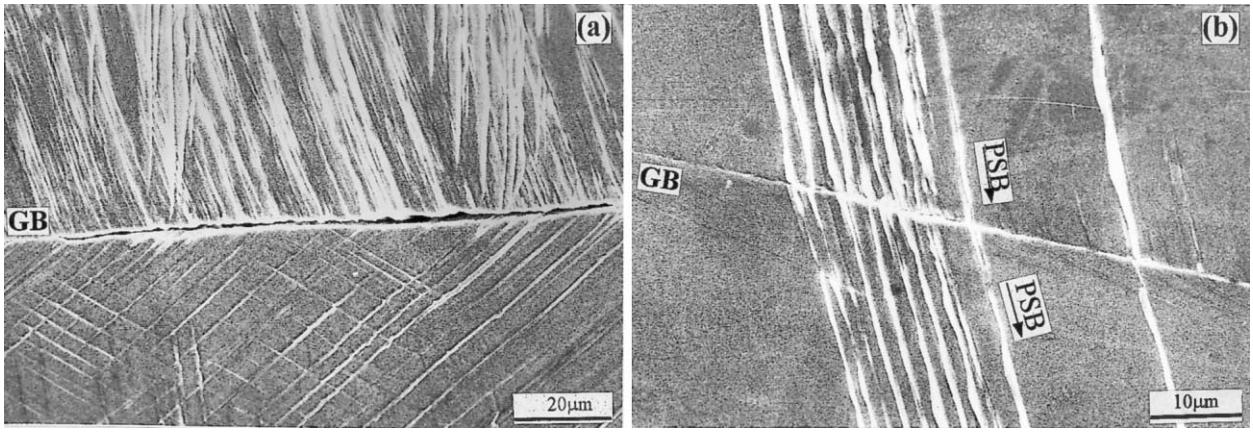

Fig. 13. (a) Fatigue cracking at B (see Fig. 12); (b) no fatigue cracking along GB segment DEF(see Fig. 12).

stress–strain behavior similar to that of a coarse-grained Cu. This systematic variation in the cyclic stress–strain response among the four studied bicrystals can be well explained by the difference in orientations of component crystal.

For a perpendicular GB bicrystal, two component crystals G1 and G2 are combined together serially. The two components are subjected to a same applied stress when the bicrystal is applied under a external stress σ_B. However, the resolved shear stress τ_{G1}, and τ_{G2} acting on the primary slip plane of each component will be different, depending on the Schmid factor Ω_{G1} and Ω_{G2} that is

$$\tau_{G1} = \sigma_B \Omega_{G1}, \qquad \tau_{G2} = \sigma_B \Omega_{G2} \tag{5}$$

As is well known, the single-slip-oriented single crystal always exhibits a clear plateau on its CSS curve. In the four groups of bicrystals studied in the present work, each at least contains a single-slip-oriented single crystal (see Fig. 6b). If the resolved shear stress of the single-slip-oriented crystal in each bicrystal is calculated by using Eq. (5), the results can be shown in Fig. 7b as a function of axial plastic strain amplitude. By comparing Fig. 7b with Fig. 7a, it is clearly seen that the softer component in the perpendicular GB bicrystal plays a dominant role for the feature of the CSS curve of bicrystal with a perpendicular GB. Fig. 8 schematically illustrates the contribution of the CSS curve of each component crystal in a bicrystal to the experimentally observed CSS response and the resulting behavior as a whole.

3.3. Interaction of persistent slip bands with grain boundaries

Under fatigue loading, GBs usually act as barriers against slip deformation and act as fatigue crack nucleation sites. These are referred to as some localized events, such as the interaction of PSBs with GBs, and are regarded as a critical factor leading to fatigue damage. However, there have been very limited reports in this respect. To the best of our knowledge, there is almost no TEM evidence clearly showing the interaction of PSB ladder structures with GBs. Recently, the electron channelling contrast (ECC) technique in SEM has been successfully applied to study the dislocation patterns, especially those induced by cyclic deformation [11]. The ECC technique can reveal some information which is difficult to obtain by the conventional TEM technique. For example, it allows the observation of dislocation configurations over the whole cross-section of the specimen, and especially at some special sites, such as the vicinity of GBs, deformation bands and crack tips. Furthermore, it is a non-destructive technique to trace the development of dislocation structures during cyclic deformation. Herein, we will mainly dis-

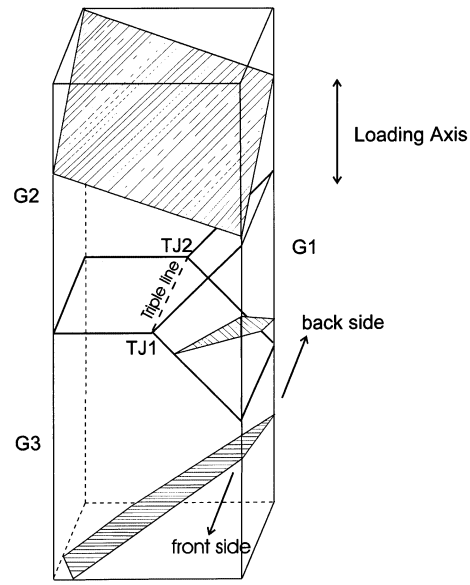

Fig. 14. Schematic illustration of the studied tricrystal and the primary slip plane in each grain.

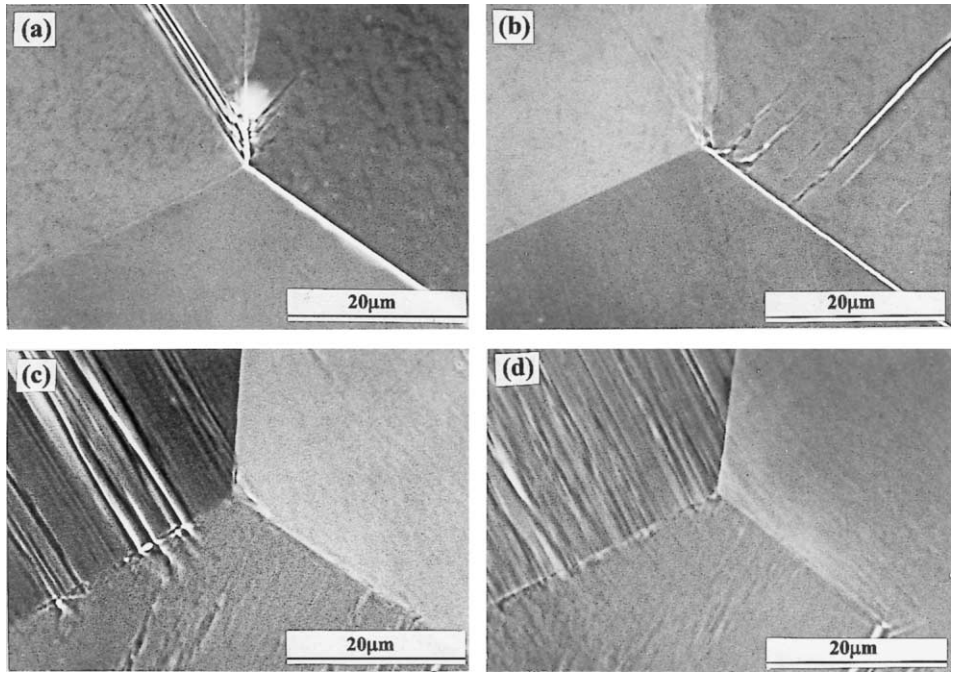

Fig. 15. Surface morphologies in the vicinity of TJ at various strain amplitudes (a) $\varepsilon_{pl} = 7 \times 10^{-4}$; (b) $\varepsilon_{pl} = 1.0 \times 10^{-3}$; (c) $\varepsilon_{pl} = 1.5 \times 10^{-3}$ and (d) $\varepsilon_{pl} = 2.0 \times 10^{-3}$.

cuss the interactions of PSBs with GBs in Cu bicrystals using this technique.

Columnar Cu crystals with low-angle (less than 5°) GBs were grown. It can be seen from Fig. 9a that all the PSBs induced by cyclic deformation can pass through the GBs continuously without activating any additional slip. It seems that low-angle GBs provide actually no resistance to PSBs. Fig. 9b illustrates the interaction of PSBs with a large-angle GB within bicrystal [$\bar{5}$ 9 1 3]/[$\bar{5}$ 7 9]. The PSBs in the softer grain [$\bar{5}$ 9 1 3] are visible, but stop at the GB and cause affected zones in the adjacent grain [$\bar{5}$ 7 9].

The primary slip planes within grains on both sides of the GB are seldom coplanar. As a natural consequence, slip is often unable to pass through the GB from one grain to another as usually observed. We fortunately produced a [$\bar{1}$ 3 4]/[1 8 $\bar{2}$ 7] Cu bicrystal with $\Sigma = 19b$ coincidence GB and the primary slip planes of the two crystals G1 and G2 in this bicrystal are coplanar except a 13.8° deviation between the primary Burgers vector $\mathbf{b}_1$ and $\mathbf{b}_2$. It is widely accepted that the PSB lamellae are embedded in matrix veins throughout the whole specimen. It may be possible to disclose the spatial interactions of PSBs with GB and the matrix lamellae by polishing the common primary slip plane across the GB layer by layer of this specially produced bicrystal, if ECC technique is adequately used. The dislocation structures induced by cyclic straining on the common primary slip plane were investigated by ECC technique. At first, as shown in Fig. 10a, the typical dislocation vein structure with some parallel and dislocation-free channels was observed. In particular, those veins almost cover the whole observed area with no dislocation walls to be seen. However, when the common primary slip plane was further polished for several layers, another structure characterized by PSB ladders embedded within the matrix veins was disclosed, as shown in Fig. 10b. After the specimen was further polished to a certain distance, a grain boundary-affected zone (GBAZ) of the dislocation patterns was revealed. Such a GBAZ appears in both G1 [$\bar{1}$ 3 4] and G2 [1 8 $\bar{2}$ 7] grains (see Fig. 11a). However, with polishing approaching to the specimen center, the GBAZ gradually disappears, as shown in Fig. 11b. The formation mechanism of the GBAZ is still not clear and needs to be further clarified.

The layer-by-layer observation on the common primary slip plane shows that most of the PSBs within the two grains do not have a one-to-one correlation across the GB even though the slip plane is coplanar (see Fig. 11c and d). The possible reason is that the Burgers vectors $\mathbf{b}_1$ and $\mathbf{b}_2$ on the common primary slip plane across the GB is not completely coincident, but deviate with an angle of 13.8° from each other.

3.4. Fatigue crack nucleation along GBs

Crack initiation along GBs in polycrystals of pure metals is often observed under either high-strain or low-strain fatigue. Kim and Laird [12,13] developed a step-mechanism for intergranular fatigue crack nucleation under high-strain fatigue. Mughrabi et al. [14]

proposed a PSB–GB interaction mechanism for intergranular fatigue cracking under intermediate and low-strain fatigue. By using bicrystals, some of our previous work indicated that fatigue cracks always initiate at the GB in spite of the GB being parallel, perpendicular to the loading axis, or inclined to the loading axis [15,16]. In general, GBs can be classified into large- and low-angle type. The susceptibility of GBs to cracking was extensively studied.

To clarify the susceptibility of large- and low-angle GBs to fatigue cracking, a special copper crystal was grown. In this crystal, several small grains G_E with misorientation less than 3° in between were embedded. But the matrix grain G_M forms large-angle GBs with these G_E. Fatigue specimens made from this specially designed crystal were subjected to cyclic deformation in the usual way.

Fig. 12 shows the whole scene of the slip morphology of the cyclically saturated crystal. The primary slip system in both the matrix crystal G_M and embedded crystal G_E were activated. However, the slip pattern along the GB surrounding G_E is different. For example, some secondary slip lines were activated along the GB segment ABC and no slip bands of G_E were able to pass through this segment. However, the well-developed slip bands within G_E can transfer through the GB segment DEF continuously. The measurement using the EBSP technique confirmed that the GB segment DEF belongs to the low-angle type, whereas the GB segment ABC has a large-angle type. It is clear from these observations that large-angle GB often stimulates the operation of secondary slip, but the slip bands can transfer through the low-angle GB with no secondary slip activated.

Careful SEM observations disclosed no fatigue cracking along the slip bands either within G_M or G_E. However, fatigue cracks can be clearly seen along the large-angle GB segment ABC (see Fig. 13a, as an example). In contrast, there was no clear fatigue crack seen along GB segment DEF (Fig. 13b). It seems that the low-angle GB is not vulnerable to fatigue loading. Based on the concept of residual dislocations and vacancies left at the GB, a simple model has been suggested to explain the difference in fatigue cracking between large- and low-angle GB [17].

4. Fatigue crack nucleation at triple junction (TJ) in Cu tricrystals

The grain boundary triple lines (TL) and junctions (TJ) occupy a large volume fraction in polycrystals and play an important role during fatigue, especially for those with fine or ultra-fine grains. However, owing to the difficulties of crystal growth, few fatigue tests have been performed on tricrystals. In the present work, a copper tricrystal ingot was grown from OFHC copper of 99.999% purity by the Bridgman method. Fig. 14 illustrated the tricrystal spark cut from an as-grown ingot and its containing primary slip planes in each grain. When the specimen was cycled at lower-strain amplitudes ($\gamma_{pl} < 10^{-4}$) to saturation, only the primary slip system was activated in all three grains and in the vicinity of TJ. While at higher-strain amplitudes, primary and secondary slip systems were both activated in the vicinity of triple junctions. As shown in Fig. 15a there is a microcrack at TJ even at a strain amplitude $\varepsilon_{pl} = 7 \times 10^{-4}$, though slip traces has not become pronounced. When the applied strain amplitude becomes higher ($\gamma_{pl} > 10^{-3}$), more slip systems are activated and slip traces become more uniformly distributed. Fatigue microcracks initiated either at TJ or along one of the three GBs in the tricrystal. According to the present study, it is suggested that the TJ may have two effects. At low-strain amplitude, the internal stresses due to the plastic strain incompatibility may retard the primary slip systems in the three grains to operate and the area near TJ can be regarded as a hard zone. At high-strain amplitude, the internal stress causes multiple slip around TJ and the primary slip traces distribute homogeneously. In this case, microcracks may nucleate at TJ due to the accommodation of vacancies generated by the annihilation of positive and negative edge dislocations. This process is different from the wedge-shaped crack at the boundary node in copper and copper–aluminum alloy tricrystals during high temperature creep [18].

5. Concluding remarks

Based on the experimental results and discussion above, the following concluding remarks can be drawn: (1) The cyclic stress–strain response characteristics of Cu crystals and their associated dislocation structures strongly depend on their location in the standard stereographic triangle. A systematic and comprehensive diagram for both the CSS curve and microstructural variations has been provided separately; (2) Grain boundaries play significant roles in fatigue damage. The extent of GBs fatigue damage depends on several factors. Among them, the most decisive ones are the orientation of the component crystal and the GB orientation with respect to the loading axis. Large-angle GBs obstructing the passage of PSBs are common phenomena and thus show a strong effect on fatigue damage; (3) The triple junction (TJ) is the least studied component in polycrystalline materials. When the grain size in materials approaches the nanoscale, the triple junction will play an even more important role in the material processing and properties. The preliminary, present work disclosed that at low-strain amplitude, primary

slip traces are retarded near the TJ, while at high-strain amplitude, they distribute homogeneously around the TJ. Fatigue cracks often nucleated at the TJ at higher-strain amplitudes. The mechanism for cracking may be different from that observed for high temperature creep.

Acknowledgements

This work was subsidized with the special funds for the Major State Basic Research Projects under Grant No. 019990650. The authors are grateful for this support.

References

[1] H. Mughrabi, Mater. Sci. Eng. 33 (1978) 207.
[2] A.S. Cheng, C. Laird, Mater. Sci. Eng. 51 (1981) 111.
[3] N.Y. Jin, Phil. Mag. A48 (1983) L33.
[4] N.Y. Jin, A.T. Winter, Acta Metall. 32 (1984) 989.
[5] T.K. Lepisto, P. Kettunen, Mater. Sci. Eng. 83 (1987) 1.
[6] C.E. Feltner, C. Laird, Acta Metall. 15 (1967) 1621 and 1633.
[7] C. Laird, in: R.W. Cahn, P. Haasen (Eds.), Physical Metallurgy, vol. 3, 4th ed., North Holland, Amsterdam, 1996.
[8] Y.D. Chuang, H. Margolin, Metall. Trans. 4A (1973) 1905.
[9] P. Peralta, C. Laird, Acta Mater. 45 (1997) 3029.
[10] P. Peralta, C. Laird, Acta Mater. 46 (1998) 2001.
[11] B. Gong, Z. Wang, D. Chen, Z.G. Wang, Scripta Mater. 37 (1997) 1605.
[12] W.H. Kim, C. Laird, Acta Metall. 26 (1978) 777.
[13] W.H. Kim, C. Laird, Acta Metall. 26 (1978) 789.
[14] H. Mughrabi, F. Ackermann, K. Herz, ASTM STP 811 (1983) 5.
[15] Y.M. Hu, Z.G. Wang, J. Int. Fatigue 20 (1998) 463.
[16] Z.F. Zhang, Z.G. Wang, S.X. Li, Fatigue Fract. Eng. Mater. Struct. 21 (1998) 1307.
[17] Z.F. Zhang, Z.G. Wang, Mater. Sci. Eng. A284 (2000) 285.
[18] S. Onaka, F. Tajima, S. Hashimoto, S. Miura, Acta Metall. 43 (1995) 307.